ChemComm



COMMUNICATION

View Article Online



Cite this: Chem. Commun., 2022, **58**. 13728

Received 13th November 2022, Accepted 22nd November 2022

DOI: 10.1039/d2cc06128g

rsc.li/chemcomm

Validation of a post-radiolabeling bioconjugation strategy for radioactive rare earth complexes with minimal structural footprint†

Raphael Lengacher, Alexia G. Cosby, Dariusz Śmiłowicz and Eszter Boros 🕩 *

The nine-coordinate aza-macrocycle DO3Apic-NO2 and its kinetically inert rare earth complexes [M(DO3A-pic-NO₂)] (M = La, Tb, Eu, Lu, Y) can be readily bioconjugated to surface accessible thioles on peptides and proteins with a minimal structural footprint. All complexes express thioconjugation rate constants in the same order of magnitude $(k = 0.3 \text{ h}^{-1})$ with the exception of Sc $(k = 0.89 \text{ h}^{-1})$. Coupling to peptides and biologics with accessible cysteines also enables postradiochelation bioconjugation at room temperature to afford injection-ready radiopharmaceuticals as demonstrated by formation of [177Lu][Lu(DO3Apic-NO₂)] and [86Y][Y(DO3Apic-NO₂)], followed by post-labeling conjugation to a cysteine-functionalized peptide targeting the prostate specific membrane antigen. The 86Y-labeled construct efficiently localizes in target tumors with no significant offtarget accumulation as evidenced by positron emission tomography, biodistribution studies and metabolite analysis.

Emerging radioactive rare earth isotopes such as 177 Lu (β^- (max) = 501 keV, $t_{1/2} = 6.64$ d), 86 Y (β^+ (max) = 4.2 MeV, $t_{1/2} = 14.7$ h), and $^{44/47}$ Sc (44 Sc: β^+ (max) = 2.6 MeV, $t_{1/2}$ = 3.97 h; 47 Sc: β^- (max) = 600 keV, $t_{1/2}$ = 3.35 d) offer promising avenues for the development of diagnostic and therapeutic radiopharmaceuticals. Additionally, their stable isotopologues are well suited for the introduction of spin-tags (Gd)²⁻⁴ and luminescence markers (Tb, Eu, Sm).⁵ However, on their own, they possess no ability to localize in specific tissues of interest and must therefore be appended to targeting vectors that enable accumulation in sites of interest. Biological targeting vectors such as peptides, monoclonal antibodies, antibody fragments, or affibodies are of specific interest due to their high target specificity; a plethora of bioconjugated radionuclides have been reported and several have been approved for routine clinical use.⁶

However, the incorporation of these isotopes into thermally sensitive biomolecules can be challenging. The most common

Department of Chemistry, Stony Brook University, 100 Nicolls Road, Stony Brook, NY 11794, USA. E-mail: eszter.boros@stonybrook.edu

approach is the incorporation of a chelator in a first step, followed by coordination to the desired radiometal in a second, penultimate step. 7-10 This works well for chelator-radionuclide pairs that form readily and rapidly at room temperature. Such systems frequently exhibit poor long-term kinetic inertness which can lead to loss of the radiometal in vivo prior to deposition in the target tissue. Alternatively, more kinetically inert systems can be employed but because these require temperatures above 40 °C for efficient radiolabeling, compatibility with the thermally sensitive nature of biologics is diminished (Fig. S2, ESI†). 11,12 A possible solution is to employ postlabeling bioconjugation strategies, which involves preformation of a thermodynamically stable and kinetically inert radiochemical complex at elevated temperature, followed by its conjugation to the targeting vector under comparatively mild conditions. This requires (1) bioconjugation reactions with fast kinetics, to minimize radioactive decay during the radiosynthetic process and (2) the functionalization of the biomolecule with the corresponding bioconjugation partner prior to the actual bioconjugation reaction. While this approach has been successfully validated using a metal-chelate functionalized tetrazine and trans-cyclooctene appended antibodies, the limited long-term stability and hydrophobicity of tetrazines can pose challenges. 13

Here, we address these shortcomings by bioconjugation of kinetically inert rare earth complexes that do not require prior functionalization of the targeting vector and retain a minimal structural footprint and high complex hydrophilicity. To this end, we explored the selective thioreactivity of nitropyridine and nitropicolinate lanthanide complexes inspired by the 8coordinate DO3A-pyr-NO2 system established by Butler and Parker. 14-17 We proposed that this reaction was well suited for a post-labeling conjugation strategy to append kinetically inert, radioactive, rare earth complexes to reactive, native thiols present on peptides and biologics. We validated this hypothesis by synthesis and characterization of select rare earth complexes of the 9-coordinate chelator DO3A-pic-NO2 and profile their reactivity for thioconjugation, radiochemical labeling efficiency

[†] Electronic supplementary information (ESI) available: Chemical synthesis, characterization, and relevant experimental details for radiolabeling and animal work are provided. See DOI: https://doi.org/10.1039/d2cc06128g

Communication ChemComm

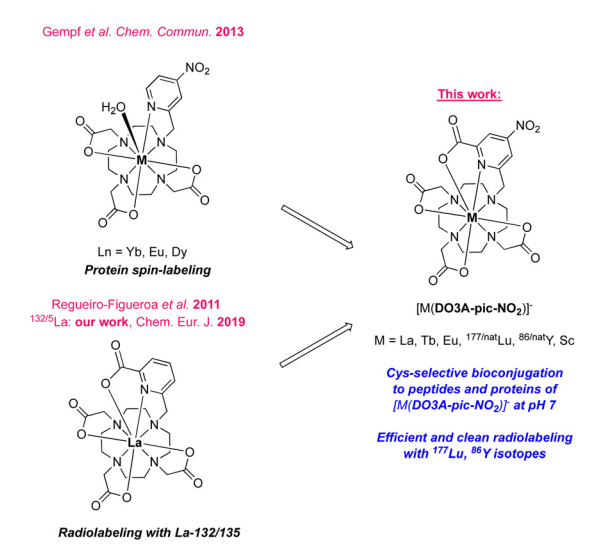


Fig. 1 Summary of the work presented in this article in context of prior art. [M(DO3A-pic-NO2)] can be readily radiolabeled and subsequently conjugated to cysteine residues of peptides/proteins at pH 7 and 37 °C, producing ready-to-inject radiopharmaceuticals.

and subsequent, direct in vivo administration for targeted PET imaging (Fig. 1).

The chemical synthesis of DO3A-pic-NO2 was adapted from literature procedures for nitropicolinate-functionalized chelators. 4,15,18 Chelation of DO3A-pic-NO2 was conducted using M^{3+} salt (M = La, Eu, Tb, Lu, Y, Sc) to produce [M(DO3A-pic-NO2)]⁻.

Next, we probed the kinetics of thioether formation using thiol ethyl thioglycolate (HS-R₁, HSEtCOOEt) at 1:1 complex to thiol ratio (Fig. 2A). Thioether formation was monitored a characteristic shift in the UV absorbance from 300 nm to 280 nm (Fig. S5, ESI†).15 We observed no significant difference for the conjugation rate among different rare earth complexes probed, with the exception of [Sc(DO3A-pic-NO₂)] $(k = 0.89 \text{ h}^{-1}, t_{1/2} = 1.1 \text{ h})$, all k-values fall into the same range and order of magnitude of 0.3 h^{-1} ($t_{1/2}$ = 3.3 h) (Fig. 2B and Table S1, ESI†). Characterization of the photophysical properties of [Tb(DO3A-pic-NO₂)] and [Tb(DO3A-pic-SEtCOOEt)] was also conducted (Table S2, ESI†) to affirm no inner sphere hydration of the corresponding coordination complexes.

To probe the scope of reactivity, we also tested conjugation to cysteine thioles using a cysteine-functionalized tetra-peptide HS-Cys-PSMA (HS-R₂) and bovine serum albumin (HS-R₃, BSA), which possesses a single, reactive cysteine residue, Cys34. Both biomolecules were conjugated successfully as indicated by chromatographic and mass spectrometric analysis (Fig. S4 and S13-S15, ESI†).

Next, we tested DO3A-pic-NO2 for radiochemical applications with ¹⁷⁷Lu and ⁸⁶Y using a post-radiolabeling conjugation approach (Fig. 3A). Quantitative labeling was achieved for 0.25-0.5 nmol of DO3A-pic-NO₂ (25 mM NH₄OAc buffer at pH = 5.5) in 15 min at 80 °C (Fig. 3B), producing an apparent molar activity of 0.248 mCi nmol⁻¹ for ¹⁷⁷Lu and 0.022 mCi nmol⁻¹ for 86Y (Fig. S8, ESI†). Complex identity was confirmed by coinjection with the isolated ^{nat}Lu/^{nat}Y species (Fig. S9, ESI†).

Freshly prepared solutions of [177Lu][Lu(DO3A-pic-NO₂)] and [86Y][Y(DO3A-pic-NO₂)] were cooled to room temperature and incubated with 6-30 equivalents of cysteine functionalized PSMA targeting peptide HS-Cys-PSMA (HS-R2, see ESI†). The reaction was conducted at pH 7.5 and 37 °C in presence of tris(2-carboxyethyl)phosphine (TCEP,1.25 eq.) to prevent the formation of disulfide bonds (Fig. 3A). The reaction achieved 69% conversion after 4 h (Fig. S12 and S14, ESI†) for [177Lu][Lu-(DO3A-pic-S-Cys-PSMA) and 54% conversion after 10 h (Fig. 3B) for $[^{86}Y][Y(DO3A-pic-S-Cys-PSMA)]^-$. To demonstrate the feasibility of a direct bioconjugation to injection approach, [86Y][Y(DO3A-pic-S-Cys-PSMA)] containing unreacted [86Y][Y(DO3A-pic-NO₂)] was administered without further purification to mice bearing bilateral xenografts with or without PSMA expression. PET imaging at 90 min post injection (Fig. 3C) and biodistribution analysis at 2 h (Fig. 3D) showed rapid, renal clearance, statistically significant target tumor uptake (6.1% ID g⁻¹, Fig. 3D, pink bars) and no notable off-target accumulation indicative of radiometal dissociation. Analysis of urine metabolites showed presence of [86Y][Y(DO3A-pic-S-Cys-PSMA)] (Fig. 3B, bottom trace). A corresponding control biodistribution experiment with [86Y][Y(DO3A-pic-NO2)] showed low accumulation in all analyzed organs and no target-specific accumulation in the tumor (0.2% ID/g, Fig. 3D, grey bars), demonstrating that the post-labeling conjugation approach produced a functional, targeted imaging agent with high kinetic inertness and efficacy. Of note, all ¹⁷⁷Lu and ⁸⁶Y labeled complexes

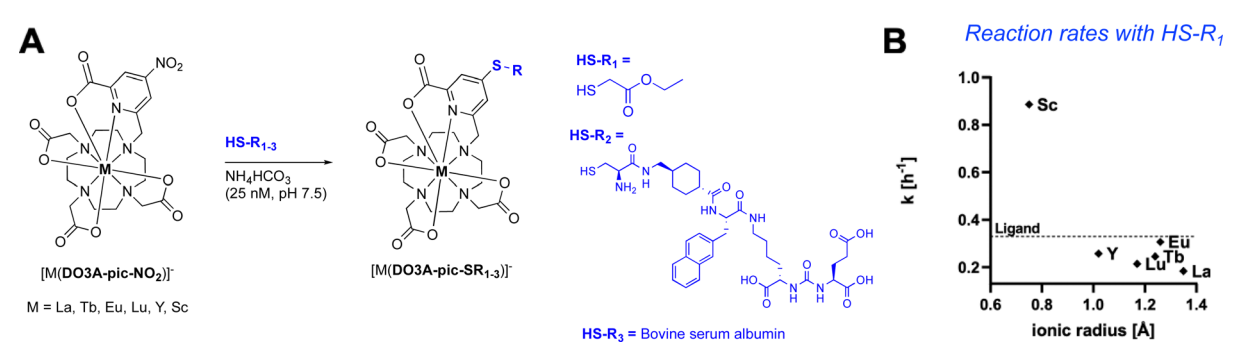


Fig. 2 (A) Reaction scheme of the thioconjugation between [M(DO3A-pic-NO2)] and HS-R1-3, resulting in the formation of [M(DO3A-pic-SR1-3)] complexes characterized in this work at r.t. in ammonium bicarbonate buffer at pH 7.5. (B) Plot of k-values $[h^{-1}]$ versus ionic radii $[\mathring{A}]$ of the employed M^{3+} ions demonstrating that ligand and corresponding complexes exhibit comparable reaction rates except for M = Sc.

ChemComm Communication

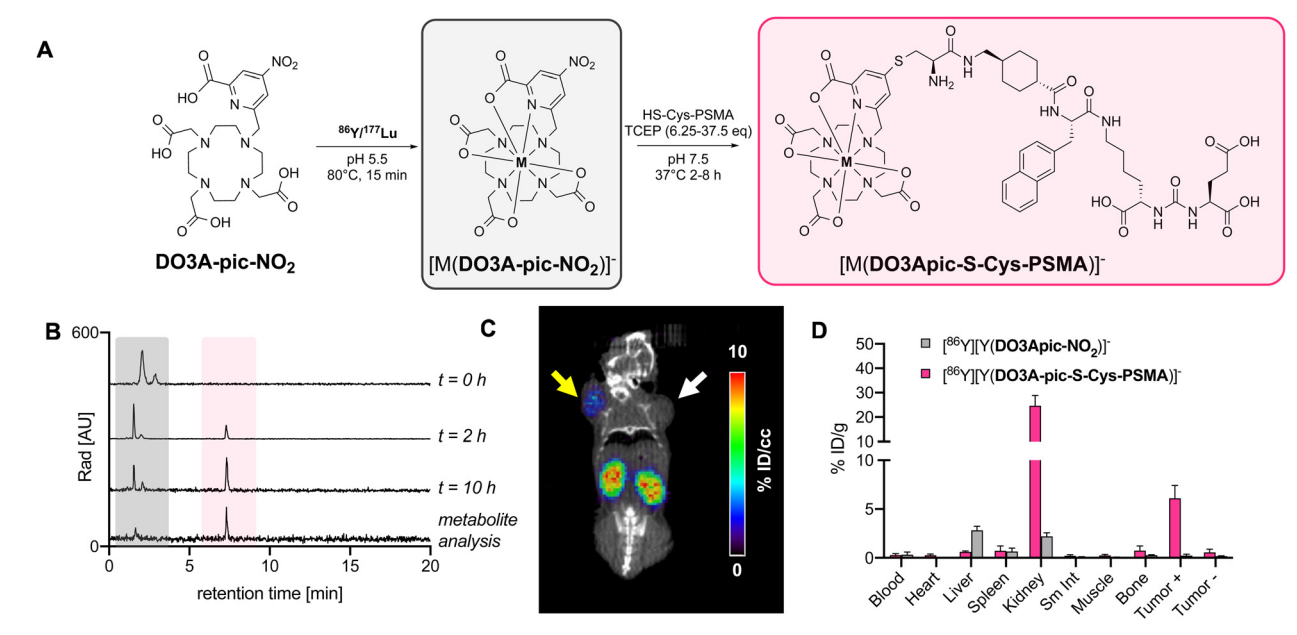


Fig. 3 (A) Reaction scheme for the radiolabeling of DO3A-pic-NO2 and subsequent thioconjugation. (B) RadioHPLC monitoring of the reaction progress for the formation of $[^{86}Y][Y(DO3A-pic-S-Cys-PSMA)]^-$ at = 2 and 10 hours – urine metabolite analysis indicates that the complex is stable in vivo. (C) Coronal PET image of [86Y][Y(DO3A-pic-S-Cys-PSMA)] 90 minutes post-injection shows target tumor uptake (yellow arrow) while PSMA-nonexpressing tumor shows no uptake. (D) Selective tumor uptake of [86Y][Y(DO3A-pic-S-Cys-PSMA)] is further affirmed by 2 h p.i. biodistribution analysis (pink) while [85Y][Y(DO3A-pic-NO₂)] shows rapid clearance and no accumulation in off-target organs (grey bars).

retained high solubility in aqueous media and did not require formulation with organic co-solvents.

Conclusively, the [M(DO3A-NO₂)] platform allows for the post-radiolabeling bioconjugation to cysteine residues at 37 °C, enabling efficient labeling of targeting vectors with a kinetically inert radiochemical 86Y/177Lu-complex for targeted in vivo imaging and therapy applications.

All authors have contributed to the manuscript. The authors acknowledge funding sources, specifically the NIH for a NIBIB R21 Trailblazer award (R21EB030071-01A1) and the National Science Foundation for an NSF CAREER (CHE 1942434).

Conflicts of interest

There are no conflicts to declare.

References

- 1 T. I. Kostelnik and C. Orvig, Chem. Rev., 2019, 119, 902-956.
- 2 L. M. Mitsumori, P. Bhargava, M. Essig and J. H. Maki, Top. Magn. Reson. Imaging, 2014, 23, 51-69.
- 3 E. C. Giese, Clin. Med. Reprod, 2018, 2, 1-2.
- 4 M. Regueiro-Figueroa, B. Bensenane, E. Ruscsák, D. Esteban-Gómez, L. J. Charbonnière, G. Tircsó, I. Tóth, A. d Blas, T. Rodríguez-Blas and C. Platas-Iglesias, Inorg. Chem., 2011, 50, 4125-4141.
- 5 J. A. Adewuyi, N. D. Schley and G. Ung, Inorg. Chem. Front., 2022, 9, 1474-1480.
- 6 D. J. Vugts and G. A. M. S. van Dongen, in Radiopharmaceutical Chemistry, ed. J. S. Lewis, A. D. Windhorst and B. M. Zeglis, Springer

- International Publishing, Cham, 2019, pp. 163-179, DOI: 10.1007/ 978-3-319-98947-1_9.
- 7 R. Rossin, P. Renart Verkerk, S. M. van den Bosch, R. C. M. Vulders, I. Verel, J. Lub and M. S. Robillard, Angew. Chem., Int. Ed., 2010, 49,
- 8 P. Adumeau, K. E. Carnazza, C. Brand, S. D. Carlin, T. Reiner, B. J. Agnew, J. S. Lewis and B. M. Zeglis, Theranostics, 2016, 6, 2267-2277.
- 9 J.-P. Meyer, J. L. Houghton, P. Kozlowski, D. Abdel-Atti, T. Reiner, N. V. K. Pillarsetty, W. W. Scholz, B. M. Zeglis and J. S. Lewis, Bioconjugate Chem., 2016, 27, 298-301.
- 10 S. M. J. van Duijnhoven, R. Rossin, S. M. van den Bosch, M. P. Wheatcroft, P. J. Hudson and M. S. Robillard, J. Nucl. Med., 2015, 56, 1422.
- 11 R. Chakravarty, S. Chakraborty, H. D. Sarma, K. V. V. Nair, A. Rajeswari and A. Dash, J. Labelled Compd. Radiopharm., 2016, **59.** 354-363.
- 12 A. Majkowska-Pilip and A. Bilewicz, J. Inorg. Biochem., 2011, 105, 313-320.
- 13 Z. Li, H. Cai, M. Hassink, M. L. Blackman, R. C. D. Brown, P. S. Conti and J. M. Fox, Chem. Commun., 2010, 46, 8043-8045.
- 14 M. Starck, J. D. Fradgley, S. Di Vita, J. A. Mosely, R. Pal and D. Parker, Bioconjugate Chem., 2020, 31, 229-240.
- K. L. Gempf, S. J. Butler, A. M. Funk and D. Parker, Chem. Commun., 2013, 49, 9104-9106.
- 16 I. D. Herath, C. Breen, S. H. Hewitt, T. R. Berki, A. F. Kassir, C. Dodson, M. Judd, S. Jabar, N. Cox, G. Otting and S. J. Butler, Chem. - Eur. J., 2021, 27, 13009-13023.
- 17 A. G. Cosby, J. J. Woods, P. Nawrocki, T. J. Sørensen, J. J. Wilson and E. Boros, Chem. Sci., 2021, 12, 9442-9451.
- 18 A. Shah, A. Roux, M. Starck, J. A. Mosely, M. Stevens, D. G. Norman, R. I. Hunter, H. El Mkami, G. M. Smith, D. Parker and J. E. Lovett, Inorg. Chem., 2019, 58, 3015-3025.